pagepress

European Journal of Histochemistry 2022; volume 66:3394

Extracellular vesicles from bone mesenchymal stem cells transport microRNA-206 into osteosarcoma cells and target NRSN2 to block the ERK1/2-Bcl-xL signaling pathway

Alimu Keremu, Pazila Aila, Aikebaier Tusun, Maimaitiaili Abulikemu, Xiaoguang Zou

Orthopedic Center, First People's Hospital of Kashgar, Xinjiang, China

ABSTRACT

Osteosarcoma (OS) is a kind of malignant tumor originating from mesenchymal tissues. Bone mesenchymal stem cells-derived extracellular vesicles (BMSCs-EVs) can play important roles in OS. This study investigated the mechanism of BMSCs-EVs on OS. BMSC surface antigens and adipogenic and osteogenic differentiation were detected by flow cytometry, and oil red O and alizarin red staining. EVs were isolated from BMSCs by differential centrifugation and identified by transmission electron microscopy, nanoparticle tracking analysis, and Western blot (WB). miR-206 and neurensin-2 (NRSN2) levels in human osteoblast hFOB 1.19 or OS cells (143B, MG-63, Saos2, HOS) were detected by RT-qPCR. Human OS cells with lower miR-206 levels were selected and treated with BMSCs-EVs or pSUPER-NRSN2. The uptake of EVs by 143B cells, cell proliferation, apoptosis, invasion, and migration were detected by immunofluorescence, 5-ethynyl-2'-deoxyuridine (EdU) and colony formation assays, flow cytometry, scratch test, and transwell assays. The binding sites between miR-206 and NRSN2 were predicted by Starbase database and verified by dual-luciferase assay. The OS xenograft model was established and treated with BMSCs-EVs. Tumor growth rate and volume, cell proliferation, and p-ERK1/2, ERK1/2, and Bcl-xL levels were detected by vernier caliper, immunohistochemistry, and WB. BMSCs-EVs were successfully extracted. miR-206 was diminished and NRSN2 was promoted in OS cells. BMSCs-EVs inhibited proliferation, migration, and invasion, and promoted apoptosis of OS cells. BMSCs-EVs carried miR-206 into OS cells. Inhibition of miR-206 in EVs partially reversed the inhibitory effect of EVs on malignant behaviors of OS cells. miR-206 targeted NRSN2. Overexpression of NRSN2 reversed the inhibitory effect of EVs on OS cells. NRSN2 activated the ERK1/2-Bcl-xL pathway. BMSC-EVs inhibited OS growth *in vivo*. In summary, BMSC-EVs targeted NRSN2 and inhibited the ERK1/2-Bcl-xL pathway by carrying miR-206 into OS cells, thus inhibiting OS progression.

Key words: Osteosarcoma; bone mesenchymal stem cells; extracellular vesicle; miR-206; NRSN2; ERK1/2-Bcl-xL.

Correspondence: Xiaoguang Zou, First People's Hospital of Kashgar, No.120 Yingbin Road, Kashgar 844000, Xinjiang, China. Tel. +86.0998.2970366. E-mail: XiaoguangZou1111@163.com

Contributions: AK, contributed to the study concepts, study design, and definition of intellectual content; PA, contributed to the literature research; AK, contributed to the manuscript preparation and XZ contributed to the manuscript editing and review; MA, XZ, contributed to the experimental studies and data acquisition; AT, contributed to the data analysis and statistical analysis. All the authors have read and approved the final version of the manuscript and agreed to be accountable for all aspects of the work.

Conflict of interest: The authors declare that they have no competing interests, and all authors confirm accuracy.

Ethics approval: All procedures were authorized by the Academic Ethics Committee of First People's Hospital of Kashgar, Xinjiang, China. The experiment was carried out in strict accordance with the guidelines for the management and use of laboratory animals issued by the Laboratory Association of China. All the laboratory procedures were used to reduce the pain of the mice.

Availability of data and materials: All the data generated or analyzed during this study are included in this published article.

Funding: This work was supported by Xinjiang Natural Science Foundation.

Introduction

Bone sarcomas are a variety of extremely rare cancers approximately representing 0.2% of all cancer types, among which the osteosarcoma (OS) is identified to be the most common malignant primary bone tumor in the skeletal system, followed by the chondrosarcoma and the Ewing sarcoma.[1] OS is a highly aggressive lesion that usually occurs at the metaphysis of the long bones and arises from mesenchymal cells, which is pathologically characterized by aberrant osteoid formation and spindle cells.[2,3]The treatment for OS is primarily based on neoadjuvant and adjuvant chemotherapy and surgical resection.[4] Up to 70% of OS patients can be long-term survivors with the surgical resection and multiagent chemotherapy, while the prognosis for patients with primary metastatic, relapsed or nonresectable OS is poor.[5] However, clinical studies evaluating targeted agents and examining modern immunotherapeutics still show disappointing results.[6] Further study is needed to understand the pathogenesis of OS, so as to provide new ideas for clinical treatment.

Mesenchymal stem cells (MSCs) are involved in the formation of the tumor microenvironment (TME) and participate in the progression of various tumors including OS through their secreted extracellular vesicles (EVs).[7] EVs are small, membranous vesicles with a diameter of 30-150 nm carrying biological macromolecules such as proteins, lipids, and RNAs.[8] EVs have important effects on regulating the crosstalk of normal and cancerous cells in TME and on regulating cell malignant behaviors *via* the cargo molecules.[9] Based on the current understanding of the pathophysiological and physiological effects of EVs, EVs are regarded as potential diagnostic markers and targeting agents for many diseases,[10] including malignant bone tumors.[11,12] Bone mesenchymal stem cells-derived extracellular vesicles (BMSCs-EVs) inhibit the OS cell malignant behaviors.[13] The deep mechanism of BMSC-EVs in the development of OS remains to be further explored.

EVs are identified to be an important tool of the intercellular communication platform due to their function of carrying microRNAs (miRNAs) and delivering them to tumor cells.[14] miRNAs act as essential regulators of OS development.[15] A variety of miRNAs are reported to function as the tumor regulators in OS, such as miR-1225-5p, miR-223-3p, miR-21, miR-421, and miR-142.[16-20] It is reported that 211 miRNAs can be detected in BMSC-EVs.[21] A large number of studies have shown that miR-206 can inhibit the progression of OS.[13,22-25] We found that miR-206 was highly expressed in EVs through EVmiRNA database. The content of miR-206 in BMSC-EVs was higher than that in BMSC-conditioned medium treated with GW4869. Therefore, we speculated that BMSC-EVs might play a role in OS progression by transporting miR-206. EV-mediated miR-101 is a tumor suppressor in OS.[26] At present, there is no report on BMSC-EVs-shuttled miR-206 in OS.

Neurensin-2 (NRSN2) is a small neuronal membrane protein located in the vesicles of nerve cells, which is highly expressed in OS and promotes the proliferation and growth of OS cells *in vivo* and *in vitro*.[27] NRSN2 can promote the proliferation, invasion, and migration of tumor cells, and play a carcinogenic role in OS. Human BMSCs-EVs target NRSN2 through miR-1913 to inhibit the progression of OS.[28] BMSCs-EVs upregulate the expressions of MALAT1 and NRSN2 and promote the proliferation, invasion, and migration of OS cells by carrying MALAT1 into OS cells.[29] NRSN2 promotes the proliferation and growth of OS cells *via* the PI3K/Akt/mTOR and Wnt/β-catenin pathway.[27] In addition, the ERK1/2-Bcl-xL pathway has been reported to play an important role in the progression of many tumors, including OS.[30] Many oncogenes promote the malignant progression of OS through the ERK1/2-Bcl-xL pathway.[31] Moreover, the phosphorylation of ERK1/2 is related to the apoptosis signal.[32] Therefore, we speculated that the ERK1/2-Bcl-xL pathway in OS cells might be activated by NRSN2. This study aims to investigate the effect and potential mechanism of BMSCs-EVs on the progression of OS by carrying miR-206.

Materials and Methods

Ethics statement

All procedures were authorized by the Academic Ethics Committee of First People's Hospital of Kashgar. The experiment was carried out in strict accordance with the guidelines for the management and use of laboratory animals issued by the Laboratory Association of China. All the laboratory procedures were used to reduce the pain of the mice.

Identification of BMSCs

The BMSCs obtained from ATCC, were subcultured in the RPMI-1640 medium, which was supplemented with 10% fetal bovine serum (FBS) in a moist incubator containing 5% CO_2 at 37°C and the medium was refreshed every 3 d. The cells were treated with 0.25% trypsin when the cells grew to 80-90% confluence. The P3 generation cells were collected and the cell adhesion and growth were observed by an inverted phase-contrast microscope. The BMSC surface positive markers CD29 (ab218273, 1/1000; Abcam, Cambridge, MA, USA), CD44 (ab218750, 1/40; Abcam), and CD71 (ab18242, 1/10; Abcam) and negative markers HLA-DR (ab64676, 9 mg/mL; Abcam), CD34 (ab223930, 1/500; Abcam), and CD45 (ab214501, 1/500; Abcam) were detected by flow cytometry and analyzed using the Cytoflex flow cytometry equipped with CytEpert 2.0 data acquisition and analysis software (Beckman Coulter, Brea, CA, USA).

Adipogenic and osteogenic differentiation of the hBMSCs were detected: i) the BMSCs were seeded in 6-well plates at 2×10^4 cells/well and cultured in the adipogenic differentiation basic medium A (Cyagen Biosciences, Guangzhou, China) for 3 d and the osteogenic differentiation basic medium B (Cyagen Biosciences) for 1 d, and the step was repeated 3 times. After fixing with 4% paraformaldehyde, the cells were stained with oil red O staining (G1262, Solarbio, Beijing, China) to observe the formation of lipid droplets under the inverted microscope (Olympus, Tokyo, Japan); ii) the BMSCs were seeded in the 6-well plates at 3×10^4 cells/well. After 4 weeks of the differentiation induction using the osteogenic medium (Cyagen Biosciences), the cells were fixed with 4% paraformaldehyde and stained with alizarin red staining (G1450, Solarbio). The calcium deposition was observed using an inverted microscope.

Isolation, identification, and grouping of BMSCs-EVs

The EVs in FBS were removed by centrifugation at 100,000g for 10 min. When the BMSCs confluence reached 80%, the supernatant was removed. Subsequently, cells were added with 10% of EVs-depleted FBS and incubated in CO_2 incubator at 37°C for 48 h. The collected supernatant was centrifuged at different speeds and the steps are as follows: at 300g at 4°C for 10 min, at 2000g at 4°C for 15 min, at 5000g at 4°C for 15 min, at 12,000g at 4°C for 30 min, and at 100,000g at 4°C for 70 min. The supernatant was removed and the sample was suspended with phosphate buffer saline (PBS). The sample was centrifuged at 100,000g at 4°C for 70 min and the supernatant was removed and the sample was suspended with PBS and then stored at -80°C. The BMSCs-EVs were identified by the following methods: i) The morphology of isolated EVs was observed using transmission electron microscopy (TEM);

ii) The EV size distribution was analyzed using nanoparticle tracking analysis (NTA); iii) Western blot (WB) was used to verify the expressions of BMSC-EVs surface positive markers CD9 (ab236630, 1/1000; Abcam), CD63 (ab134045, 1/1000; Abcam), and CD81 (ab109201, 1/1000; Abcam), and a negative marker Calnexin (ab92573, 1/20000; Abcam), and the supernatant of BMSCs added with GW4869 was used as negative control (NC). The protein quantification was determined by the bicinchoninic acid (BCA) protein quantitative kit according to the instructions. Protein content was used as the standard when EVs were used.

EVs used in this study were assigned into the following 6 groups: 1) GW group: the PBS resuspension obtained according to the same steps as the EV extraction after BMSCs were cultured with GW4869 supplemented with 10 μM EV secretion inhibitor for 2 h;[33,34] 2) EVs group; 3) RNase group: the EVs were treated with RNase (Sigma-Aldrich, St Louis, USA); 4) RNase + sodium dodecyl sulfate (SDS) group: the EVs were treated with RNase and SDS (Sigma-Aldrich); 5) EVs-NC group: EVs extracted from BMSCs transfected with inhibitor NC (100 nmol/L); and 6) EVs-inhi group: EVs extracted from BMSCs transfected with miR-206 inhibitor (100 nmol/L). MiR-206 inhibitor and its control inhibitor NC were both purchased from Biomics Biotech (Biomics Biotech, Jiangsu, China).

Cell culture and grouping

Human osteoblast hFOB 1.19 and human OS cell lines 143B, MG-63, Saos2, and HOS were obtained from ATCC cell bank (ATCC, Manassas, VA, USA). The cells were cultured in RPMI-1640 medium (HyClone, Logan, UT, USA) supplemented with 10% FBS (Thermo Fisher Scientific, Waltham, MA, USA) and 1% penicillin/streptomycin (Gibco, Grand Island, NY, USA) in a moist incubator at 37°C containing 5% CO_2. When confluence reached 70%-80%, the 143B cells were transfected with pSUPER-NRSN2 or corresponding NC according to Lipofectamine 3000 (Invitrogen, Carlsbad, CA, USA). According to the grouping, EVs were added to each group for 24-h incubation.

The 143B cell lines used in this study were assigned into the following 10 groups: 1) blank group (143B in normal culture for 24 h without treatment); 2) oe-NC group (pSUPER empty plasmid transfected into 143B and cultured for 24 h); 3) oe-NRSN2 group (NRSN2 overexpression plasmid pSUPER-NRSN2 transfected into 143B and cultured for 24 h); 4) EVs group [143B cell line was added with 100 μg/mL EVs and incubated for 24 h;[29] 5) NC group (143B cell line was added with the same amount of PBS resuspension obtained according to the same steps as the EV extraction after adding with GW4869 and cultured for 24 h); 6) EVs-NC group (143B cell line was added with 100 μg/mL EVs-NC and incubated for 24 h); 7) EVs-inhi group (143B cell line was added with 100 μg/mL EVs-inhi and incubated for 24 h); 8) oe-NRSN2 + EVs group (143B cell line was treated with 100 μg/mL EVs, transfected with oe-NRSN2 and cultured for 24 h); 9) oe-NC + EVs group (143B cell line was treated with 100 μg/mL EVs, transfected with oe-NC and cultured for 24 h); and 10) oe-NRSN2 + EVs + PD group (143B cell line was treated with 100 μg/mL EVs, transfected with oe-NRSN2, treated with 20 μM ERK/12 specific inhibitor PD98059 and cultured for 24 h.[35]

5-ethynyl-2'-deoxyuridine (EdU) assay

EdU assay was performed as described.[13] Subsequently, 5×10^3 cells were seeded into 96-well plates. EdU Apollo 567 Cell Tracking Kit (RiboBio, Guangzhou, China) was utilized for EdU determination. The percentage of EdU-positive cells was counted in three independent experiments.

EVs uptake test

The 143B cells were stained with CellTrace CFSE kit (Invitrogen, Waltham, MA, USA) according to the instructions. The PKH26 Fluorescent Cell Linker Kit (Sigma-Aldrich) was used to label EVs. A total of 1 mL of PKH26 dye solution (1:1000) was mixed with EVs containing 20 μg protein content for 20 min, and the sample was washed with PBS and centrifuged at 1000000 g for 70 min. Subsequently, PKH26 labeled EVs were added into carboxyfluorescein diacetate succinimidyl ester (CFSE) labeled cells for co-culture for 24 h. The uptake of EVs at different time points was observed using confocal fluorescence microscopy.

Flow cytometry

The cell apoptosis was tested by flow cytometry. OS cells from different treatment groups were stained with Annexin V/FITC Kit (BD Biosciences, San Jose, CA, USA). The cells were analyzed by flow cytometry.

Transwell assay

Cell migration and invasion experiments were performed using the Transwell chamber (BD Science, Bedford, MA, USA) according to the manufacturer's instructions. The 143B cells were cultured in the serum-depleted McCoy's 5A medium and cultured for 24 h. Then, the cells were trypsinized and resuspended in serum-depleted McCoy's 5A medium. The 5×10^4 cells were placed in the apical chamber of the Transwell plate and the 90% McCoy 5A medium containing 10% FBS was placed in the basolateral chamber and incubated for 24 h. The remaining cells in the apical chamber were removed with a sterile cotton swab, the migrated cells were fixed with 4% formaldehyde on the lower surface of the filter, stained with 2% crystal violet, counted, and imaged under an optical microscope. Cell invasion assay was similar to cell migration assay except that the filter membrane of Transwell apical chamber was coated with Matrigel in BioCoat Matrigel invasion kit (BD science). The cells were counted and imaged using an optical microscope.

Dual-luciferase assay

The complementary sequence of miR-206 and NRSN2 wild type (WT) 3'UTR and mutant (MUT) 3'UTR were amplified and cloned into the pMIR plasmid vector (Promega, Madison, WI, USA) to construct NRSN2-WT and NRSN2-MUT plasmids. The 143B cells were seeded in the 96-well plates at 2×10^4 cells/well overnight. The recombinant plasmids were co-transfected with miR-206 mimic and its NC (GenePharma, Shanghai, China) into the cells using the Lipofectamine 2000 (Invitrogen) and the transfection of phRL-tk was used as the control. After 48 h, the cells were washed with PBS and lysed and the luciferase activity was determined using the dual-luciferase assay kit (Promega). NRSN2-WT and NRSN2-MUT plasmids were constructed by Cobioer Biosciences Co., Ltd. (Nanjing, China).

RT-qPCR

The TRIzol (Invitrogen) was used to extract the total RNA from cells or tumor tissues. The PrimeScript RT reagent kit (Takara Biotechnology, Inc., Kyoto, Japan) was used for reverse transcription of RNA into cDNA. The TaqMan primers and probes were all from Takara. The qPCR was performed according to the ABI PRISM 7900 sequence detection system of SYBR Green II (Takara Biotechnology, Inc.). The reaction conditions were pre-denaturation at 95°C for 5 min and 40 cycles of denaturation at 95°C for 15 s, annealing at 60°C for 20 s, and extending at 72°C for 35 s. GAPDH is the internal reference for ANXA2 and U6 is the internal reference for miR-206 and the $2^{-\Delta\Delta Ct}$ method was used to analyze

gene expression. The primer sequences (synthetized by Sangon Biotech Co., Ltd., Shanghai, China) are shown in Table 1.

Western blot

The tumor tissue homogenate or cells were lysed with enhanced radio-immunoprecipitation assay (RIPA) lysate (Boster Biological Technology Co., Ltd., Wuhan, China) containing protease inhibitor for 20 min. The sample was centrifuged at 3000 g for 20 min and the supernatant was collected. The concentration of supernatant protein was detected by BCA protein quantitative kit (BOSTER). The protein was isolated by 10% SDS-PAGE. The isolated protein was transferred to polyvinylidene fluoride (PVDF) membranes, blocked with 5% bovine serum albumin (BSA) for 2 h to block nonspecific binding, and respectively incubated using the primary antibodies p-ERK1/2 (Thr202/Tyr204) (#9101S, 1:1000, CST, Beverly, MA, USA), ERK1/2 (ab184699, 1:10,000, Abcam), and Bcl-xL (ab32370, 1:25; Abcam) at 4°C overnight. After washes by tris buffered saline-Tween20 (TBST), the sample was added with horseradish peroxidase (HRP) labeled secondary antibody and incubated for 1 h. Enhanced chemiluminescence fluid (EMD Millipore, Bedford, MA, USA) was used for development. Image-Pro Plus 6.0 (Media Cybernetics Inc., Silver Springs, MD, USA) was used to quantify gray scale of the band in each group in WB images, and GAPDH (ab128915, 1/10000, Abcam) was used as internal parameters.

In vivo xenotransplantation

A total of 36 BALB/c female athymic nude mice (6-week-old) were from Beijing Vital River Laboratory Animal Technology Co., Ltd. (Beijing, China). The xenograft model of OS was established by subcutaneous injection of 5×10^6 143B cells on the right side of the mice. Mice were injected with NC and EVs (50 μg/100 μL PBS) or NC through the tail vein once every 3 days for 18 days. The length (L) and width (W) of tumor were measured with a vernier caliper every 3 d and the tumor volume was calculated according to the formula (length × width^2)/2. After the experiment, 6 were used for tumor weight measurement, 6 for immunohistochemical detection, and the other 6 for RT-qPCR and Western blot.

Immunohistochemistry

The tumor tissue sections were prepared and baked in constant temperature oven at 45°C for 3 h. After dewaxing and hydration, the sections were added with 3% H_2O_2 and placed at room temperature for 10 min to eliminate the activity of endogenous peroxidase. The sections were washed 3 times with phosphate-buffered saline with Tween-20 (PBST) and placed into citrate buffer for microwave antigen repair. The solution was heated to boiling, naturally cooled (5-10 min), repaired 3 times and the samples were dropped to room temperature. The samples were covered with goat serum and stored in a wet box at 37°C for 1 h and the sealing fluid was removed. The samples were added with Ki-67 primary antibody (ab15580. 5 μg/mL, Abcam) fluid and placed in a wet box at 4°C overnight. The next day, the samples were rewarmed to room temperature, washed with PBST 3 times, added with biotinylated secondary antibody fluid, incubated in a wet box at 37°C for 15 min, and washed with PBST 3 times.

Statistical analysis

SPSS 21.0 (IBM Corp. Armonk, NY, USA) and GraphPad Prism 8.01 (GraphPad Software Inc., San Diego, CA, USA) were used for data analysis and mapping. Kolmogorov-SmiRnov test showed that the continuous variable was in normal distribution and expressed as mean ± SD. One-way analysis of variance (ANOVA) and two-way ANOVA were used for comparison among groups. Tukey's multiple comparisons test was used for *post-hoc* test. A p-value <0.05 indicated statistical significance.

Results

Identification of BMSCs and EVs

In the process of BMSCs subculture, the senescent cells were gradually removed. After 3-4 generations of purification, relatively homogeneous and active cells were obtained. The cells were spindle-shaped and arranged in a vortex (Figure 1A). Flow cytometry was used to detect the surface antigens of BMSCs. It was found that CD29 (99.09%), CD44 (99.09%) and CD71 (99.15%) were all positive, and HLA-DR (0.03%), CD34 (0.11%) and CD45 (0.06%) were all negative (Figure 1B), indicating that the cultured cells were BMSCs. When the confluence reached 100%, BMSCs were cultured in the specific medium for adipogenic differentiation. After 72 h of culture, small lipid droplets were observed in the cells, and after another 2 h of culture, a large number of lipid droplets in the long spindle or polygonal shape were observed in the cells. The deposition of lipid components was verified by oil red O staining, suggesting the ability of lipid differentiation of BMSCs (Figure 1C). BMSCs were differentiated into osteoblasts after adding with a specific culture medium. On the 14th day of culture, the whole cells were full of calcium granules, and the cells grew in colony form. The central cells gradually fused, lost the typical cell structure, and formed transparent calcium nodules. After 4 weeks of culture, the samples were stained into red with alizarin red staining (Figure 1D). Subsequently, EVs were isolated and collected from BMSCs using ultracentrifugation. The EVs were in round or oval shape with a typical cup shape under TEM with a diameter of 60-160 nm, and the membrane structure of the EVs was observed in the periphery of the EVs (Figure 1E). To further determine their size distribution, NTA was used for analysis. It was shown in Figure 1F that EVs were mainly distributed at about 100 nm, and the concentration was 4.6×10^6/mL. It was also shown by the WB analysis that the EVs markers CD9, CD63, and CD81 were abundant in EVs, and there was no significant expression of Calnexin (Figure 1G). The results above indicated that the correct BMSCs-EVs were isolated.

Table 1. Primer sequences.

Gene	Forward 5'-3'	Reverse 5'-3'
miR-206	GGAAGAAGGAAGGGGGCG	AGTGCAGGGTCCGAGGTATT
NRSN2	CCCTTTGGAACAAGCACATT	AAAGTGGACACGGATCTTGG
GAPDH	CTCAGACACCATGGGGAAGGTGA	ATGATCTTGAGGCTGTTGTCATA
U6	ATTGGAACGATACAGAGAAGATT	GGAACGCTTCACGAATTTC

BMSCs-EVs inhibited the proliferation, migration, and invasion of OS cells

To explore the role of BMSCs-EVs in the progression of human OS, human osteoblast hFOB 1.19 and OS cells 143B, MG-63, Saos2, and HOS were cultured *in vitro*, and the level of miR-206 in each cell line was detected by RT-qPCR. The expression of miR-206 was lowered in OS cells and the miR-206 was the lowest in 143B cells (all $p<0.01$) (Figure 2A). Human OS cell 143B cells were selected for the following experiments. It was found by uptake test that EVs could be internalized by 143B cells (Figure 2B). Subsequently, the effect of EVs on the proliferation of OS cells was detected by EdU assay. It was shown that EVs inhibited OS cell proliferation significantly ($p<0.01$) (Figure 2C). OS cell apoptosis was detected by flow cytometry. It was found that OS cell apoptosis was increased clearly after BMSCs-EVs treatment ($p<0.01$) (Figure 2D). In addition, Transwell assays indicated that BMSCs-EVs could reduce OS cell invasion and migration ($p<0.01$) (Figure 2E). The results above suggested that BMSC-EVs inhibited the OS cell malignant behaviors.

BMSCs-EVs carried miR-206 into OS cells

A study has demonstrated that miR-206 plays a key role in OS morbidity and development.[36] GEO database (https://www.ncbi.nlm.nih.gov/geo/) demonstrated that the expression of miR-206 was significantly downregulated in chip GSE28423 OS samples (Figure 3A). Knockdown of miR-206 can promote the progression of OS.[22,37] High expression of miR-206 reduces the malignancy of OS cells.[38] BMSC-EVs inhibit OS progression by niR-206 targeting TRA2B.[13] Compared with the BMSCs-conditioned medium treated with GW4869, the content of miR-206 in BMSCs-EVs was significantly upregulated (Figure 3B). Therefore, we speculated that BMSC-EVs affect OS progression by transporting miR-206. After further treatment of RNase, miR-206 expression in EVs was not changed significantly, while downregulated significantly when SDS was added during RNase treatment ($p<0.01$) (Figure 3B), indicating that miR-206 was encapsulated in EVs. In addition, BMSCs were transfected using a miR-206 inhibitor to inhibit the miR-206 expression and EVs were isolated and miR-206 expression in EVs was significantly downregulated ($p<0.01$) (Figure 3C).

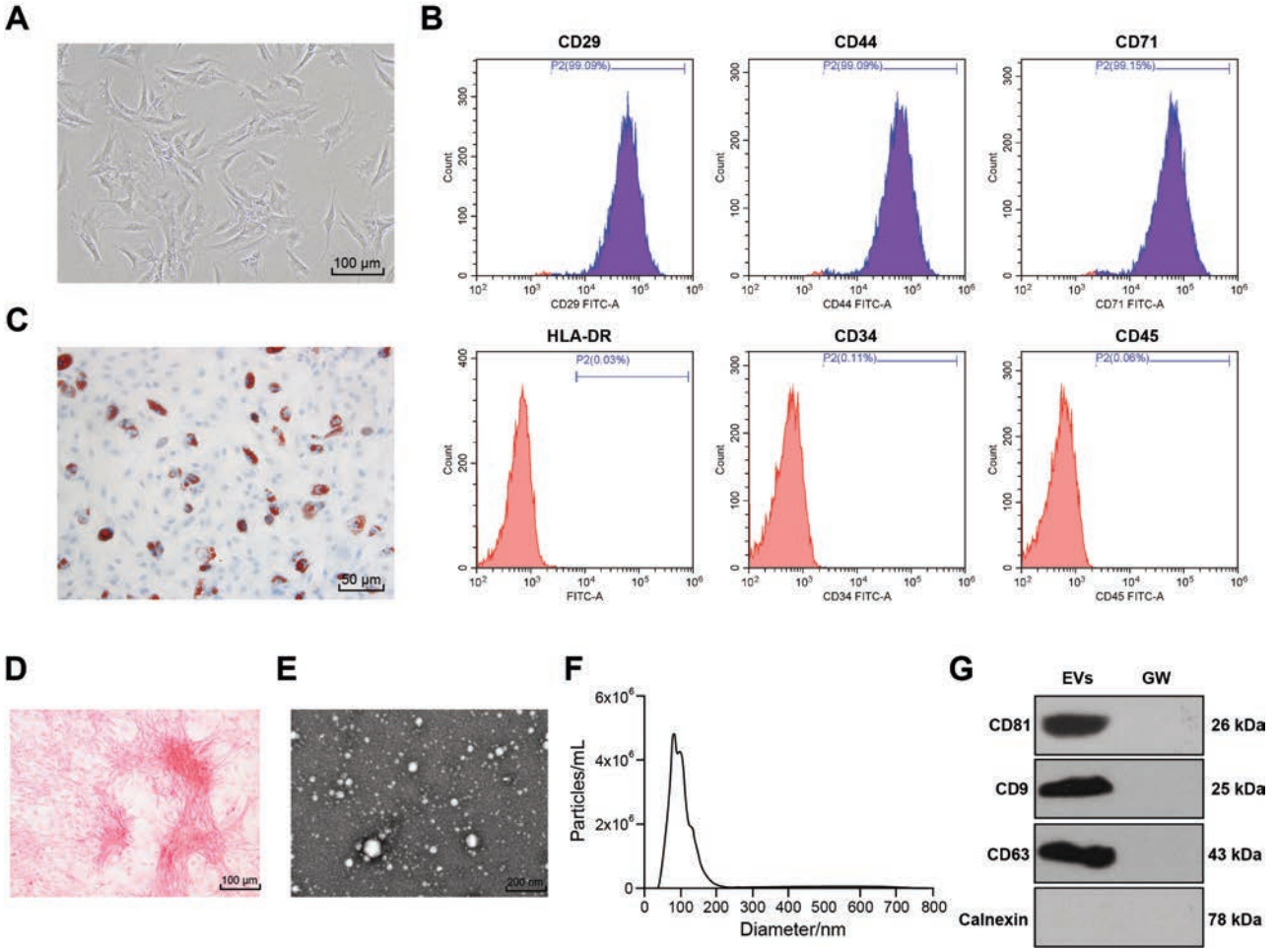

Figure 1. Identification of BMSCs and EVs. The BMSCs obtained from ATCC were subcultured. A) The morphology of BMSCs in the fourth generation was observed by microscope. B) The positive marker proteins (CD29, CD44, and CD71) were positively expressed and negative marker proteins (HLA-DR, CD34, and CD45) of BMSCs were negatively expressed detected using flow cytometry. C) Lipid differentiation was observed by oil red O staining. D) Alizarin red staining was used to observe osteogenic differentiation; the EVs were extracted. E) The morphology of BMSCs-EVs was observed with a typical cup shape by TEM. F) The size distribution of EVs was mainly at about 100 nm analyzed using NTA. G) WB detected that the expressions of EV surface CD9, CD63, and CD81 enrichment and calnexin protein were not significantly expressed.

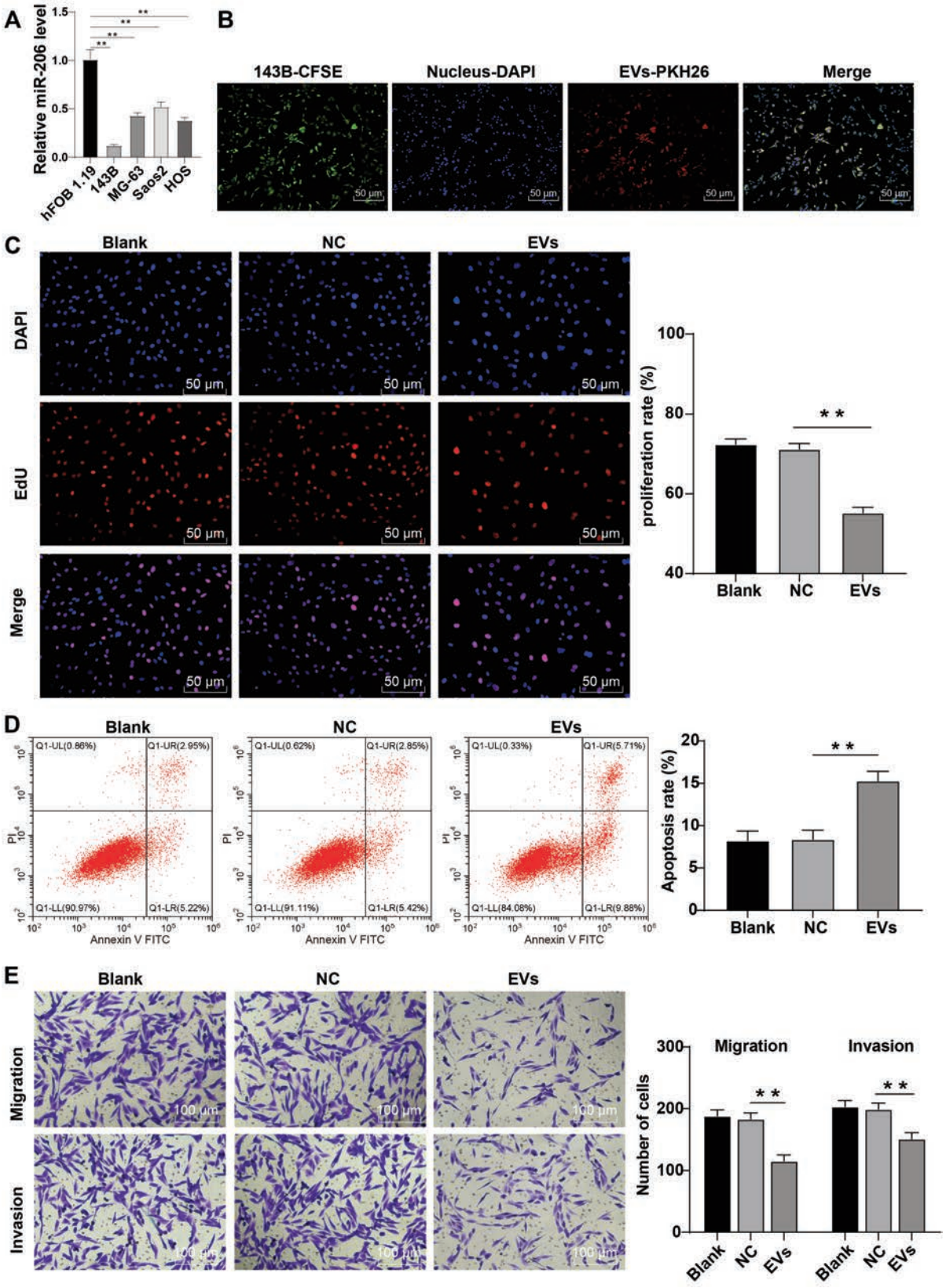

Figure 2. BMSCs-EVs inhibited the proliferation, migration, and invasion of OS cells and promoted apoptosis. Human OS cells were cultured *in vitro* and treated with EVs. A) miR-206 level in human osteoblasts hFOB 1.19 and OS cells 143B, MG-63, Saos2, and HOS was detected by RT-qPCR. B) The uptake of EVs by OS cells was detected using immunofluorescence (C) EdU assay showed that 143B cell proliferation was inhibited. D) Flow cytometry demonstrated that apoptosis was increased. E) Transwell assay showed that cell migration (above) and invasion (below) were inhibited. Three cell tests were performed and the data were expressed as mean ± SD. One-way ANOVA was used for comparison among groups. Tukey's multiple comparisons test was used for *post-hoc* test; **p<0.01.

After EVs-inhi treatment, the expression of miR-206 in OS cells was significantly downregulated compared with that in the EVs-NC group ($p<0.01$) (Figure 3D). The results above indicated that BMSCs- EVs carried miR-206 into OS cells.

Inhibition of miR-206 expression in EVs partially reversed the inhibition of EVs on malignant behaviors of OS cells

To explore whether BMSC-EVs exerted effects on OS through miR-206, EVs from different treatment groups were added to OS cells for culture and the OS cell malignant behaviors were detected. After the inhibition of miR-206 in EVs, the proliferation of OS cells was significantly increased ($p<0.01$) (Figure 4A), the apoptosis was reduced ($p<0.01$) (Figure 4B), and the migration and invasion were increased ($p<0.01$) (Figure 4C). The results above indicated that miR-206 inhibition in EVs partially reversed the inhibitory effect of EVs on malignant behaviors of OS cells, suggesting that the inhibitory effect of EVs on proliferation, migration, and invasion of OS cells was achieved by carrying miR-206 into OS cells.

miR-206 targeted NRSN2

It was confirmed by the previous study that BMSCs-derived miR-206 inhibited the malignant behaviors of OS cells. NRSN2 has been proved to be a new oncogenic protein, which can promote the proliferation of OS cells.[27] ECORI Pan-Cer database analysis manifested that there was a negative correlation between miR-206 and NRSN2 in sarcomas (SARC) (Figure 5A). In addition, the binding sites between miR-206 and NRSN2 were predicted using the Starbase database (Figure 5B). Subsequently, the targeted binding of miR-206 with NRSN2 was verified by dual-luciferase reporter assay ($p<0.01$) (Figure 5B). After miR-206 silencing, NRSN2 mRNA level in BMSCs-EVs was facilitated ($p<0.01$) (Figure 5C). Furthermore, the mRNA level of NRSN2 in each cell

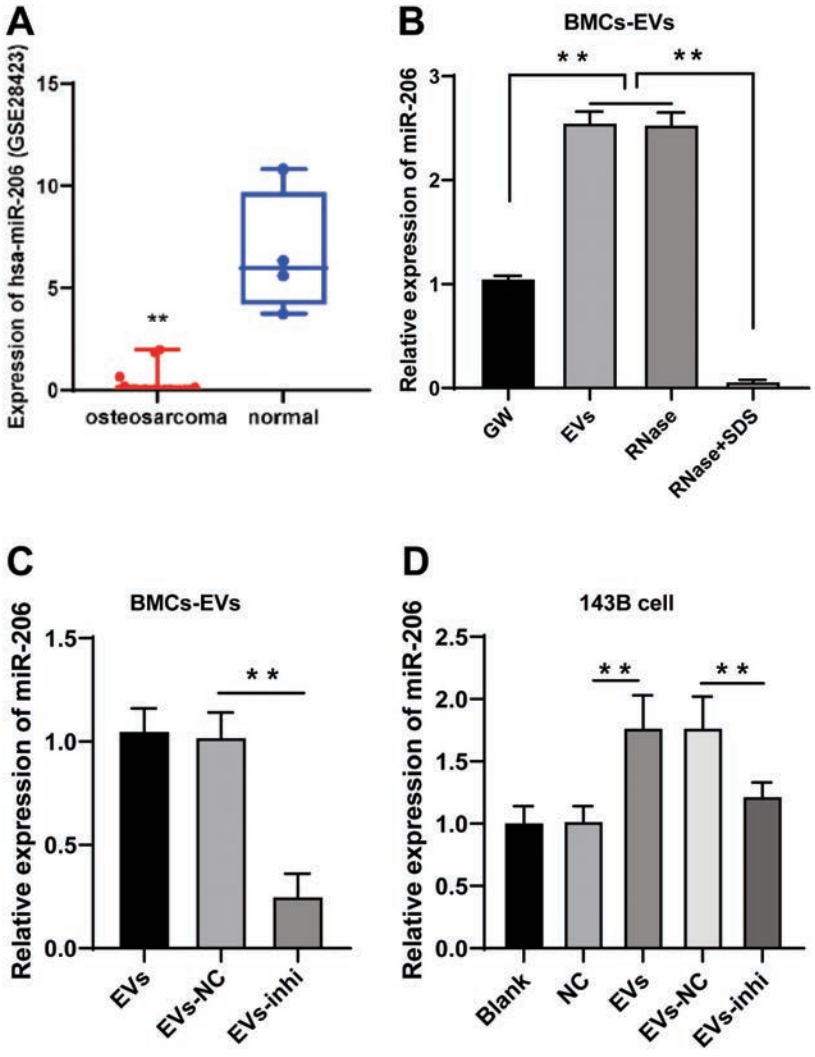

Figure 3. BMSCs-EVs carried miR-206 into OS cells. A) Bioinformatics analysis showed that the expression of miR-206 in GSE28423 OS samples was lower than that in control samples. The EVs were treated differently, and the expression of miR-206 in EVs was detected by RT-qPCR (B,C). The OS cells were treated with EVs from different groups, and the expression of miR-206 in OS cells was detected by RT-qPCR (D). Three cell tests were performed and the data were expressed as mean ± SD. Independent t-test was used for comparison between two groups in panel (A) and one-way ANOVA was used for comparison among groups in panels (B-D). Tukey's multiple comparisons test was used for *post-hoc* test; **p<0.01.

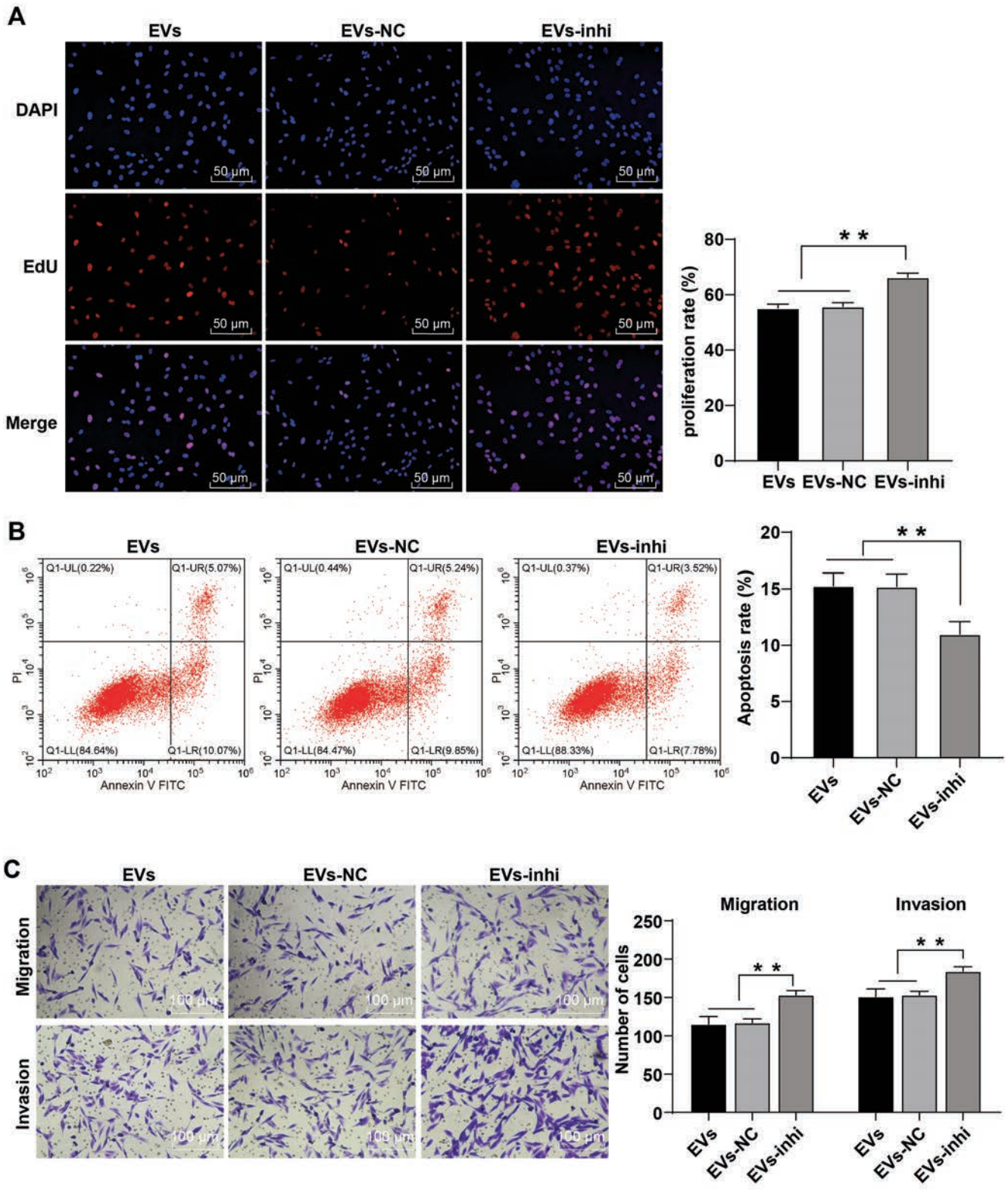

Figure 4. The inhibition of miR-206 in EVs partially reversed the effect of EVs on the proliferation, migration, and invasion of OS cells. EVs of different treatment groups were added into OS cells for culture. After miR-206 in EVs was inhibited, EdU assay showed that cell proliferation rate was increased (A); flow cytometry demonstrated that apoptosis was reduced (B); transwell assay showed that cell migration (above) and invasion (below) were increased (C). Three cell tests were performed and the data were expressed as mean ± SD. One-way ANOVA was used for comparison among groups. Tukey's multiple comparisons test was used for *post-hoc* test; **p<0.01.

line was detected. The mRNA level of NRSN2 in OS cell lines was higher than that in human osteoblasts, and the level was the highest in 143B cells (all p<0.01) (Figure 5D). Finally, the mRNA level of NRSN2 in 143B cells treated with EVs in different groups was detected. After the treatment with EVs, the expression of NRSN2 was significantly downregulated in 143B cells and upregulated when miR-206 was inhibited in EVs (all p<0.01) (Figure 5E). These results suggested that there was a negative regulatory relationship between miR-206 and NRSN2.

Overexpression of NRSN2 reversed the inhibitory effect of EVs on OS cells

Furthermore, the NRSN2 was overexpressed in OS cells during the treatment of EVs. It was found by RT-qPCR that after EVs were treated, NRSN2 mRNA level was significantly decreased in OS cells, while after NRSN2 was further overexpressed, the NRSN2level was increased in OS cells (all p<0.01) (Figure 6A). Subsequently, the OS cell malignant behaviors were detected. After the overexpression of NRSN2, proliferation was increased

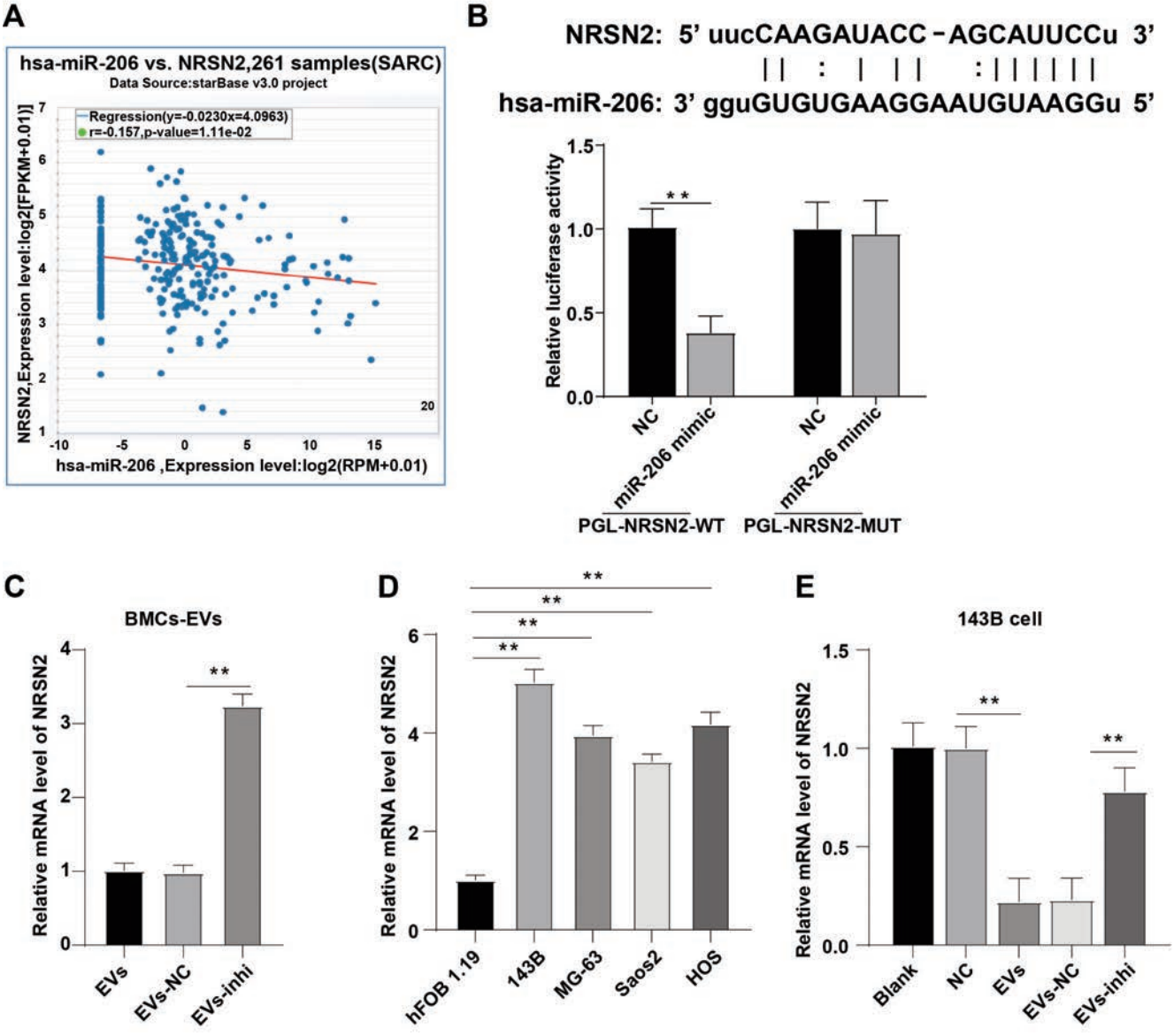

Figure 5. miR-206 targeted NRSN2. A) Pan-Cer database showed that miR-206 and NRSN2 were negatively correlated in sarcomas. B) The binding sites between miR-206 and NRSN2 were predicted using Starbase database. The targeted binding of miR-206 and NRSN2 was verified by dual-luciferase reporter assay. C-E) The NRSN2 mRNA level in BMCs-EVs/human osteoblasts hFOB 1.19 and OS cells 143B, MG-63, Saos2 and HOS/143B cells in each treatment group was detected by RT-qPCR. Three cell tests were performed and the data were expressed as mean ± SD (A). Independent *t*-test was used for comparison between two groups in (B) and one-way ANOVA was used for comparison among groups in (C-E). Tukey's multiple comparisons test was used for *post-hoc* test; **p<0.01.

(p<0.01) (Figure 6B), apoptosis was reduced (p<0.01) (Figure 6C), and cell migration and invasion were increased (all p<0.01) (Figure 6D). The results above indicated that overexpression of NRSN2 partially reversed the inhibitory effects of EVs on the cell malignant behaviors.

NRSN2 promoted OS cell proliferation, migration, and invasion by activating the ERK1/2-Bcl-xL signaling pathway

The ERK1/2-Bcl-xL pathway is important in the progression of many tumors, including OS.[30] A study has shown that the activation of the ERK1/2-Bcl-xL pathway promotes the malignant

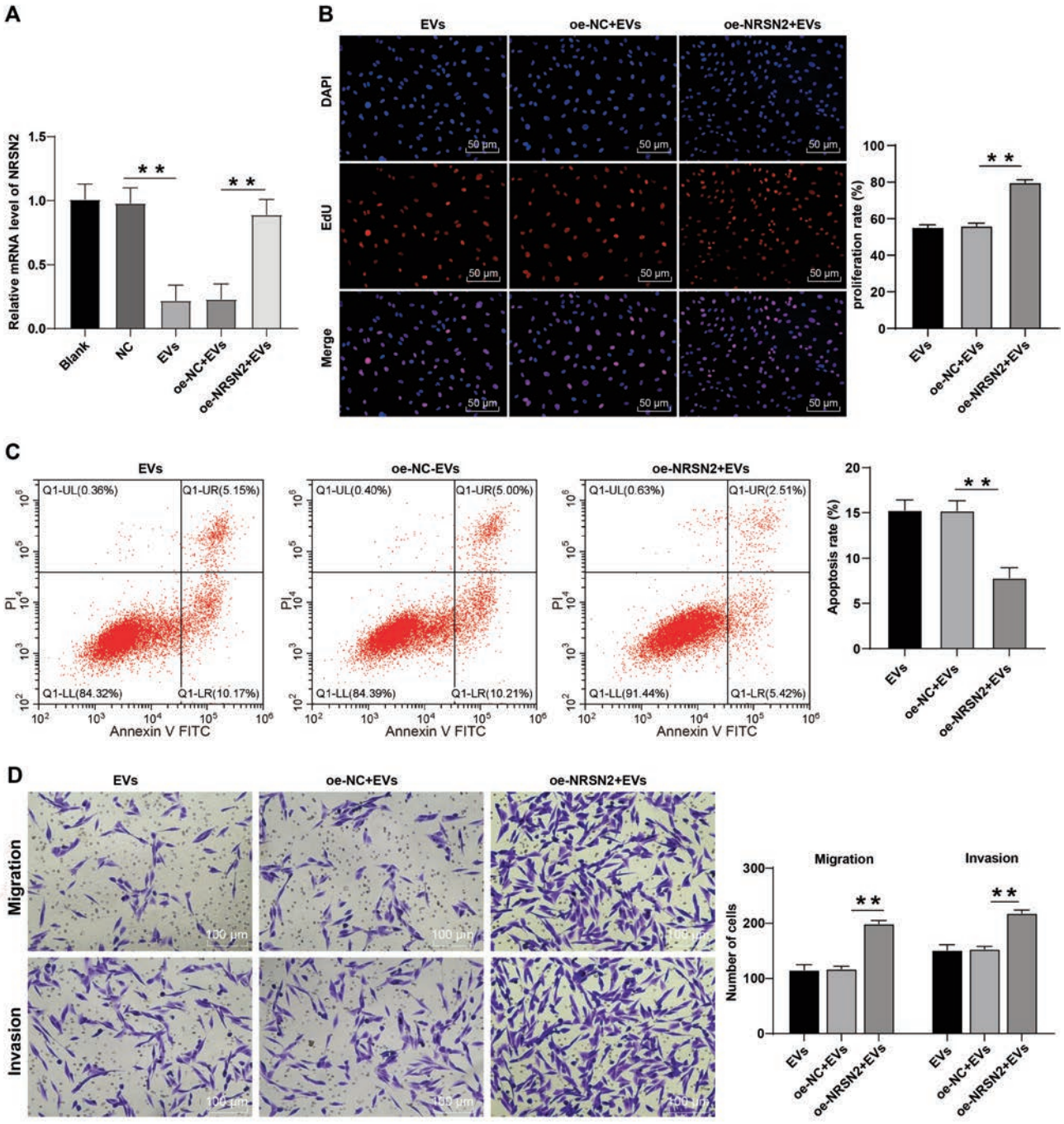

Figure 6. Overexpression of NRSN2 reversed the inhibitory effect of EVs on proliferation, migration, and invasion of OS cells. The NRSN2 was overexpressed when the OS cells were treated with EVs. A) RT-qPCR demonstrated that the level of NRSN2 mRNA was increased. B) EdU assay showed that the proliferation rate was increased. C) Flow cytometry showed that apoptosis was reduced. D) Transwell assay showed that cell migration (above) and invasion (below) were increased. Three cell tests were performed and the data were expressed as mean ± SD. One-way ANOVA was used for comparison among groups. Tukey's multiple comparisons test was used for *post-hoc* test; **p<0.01.

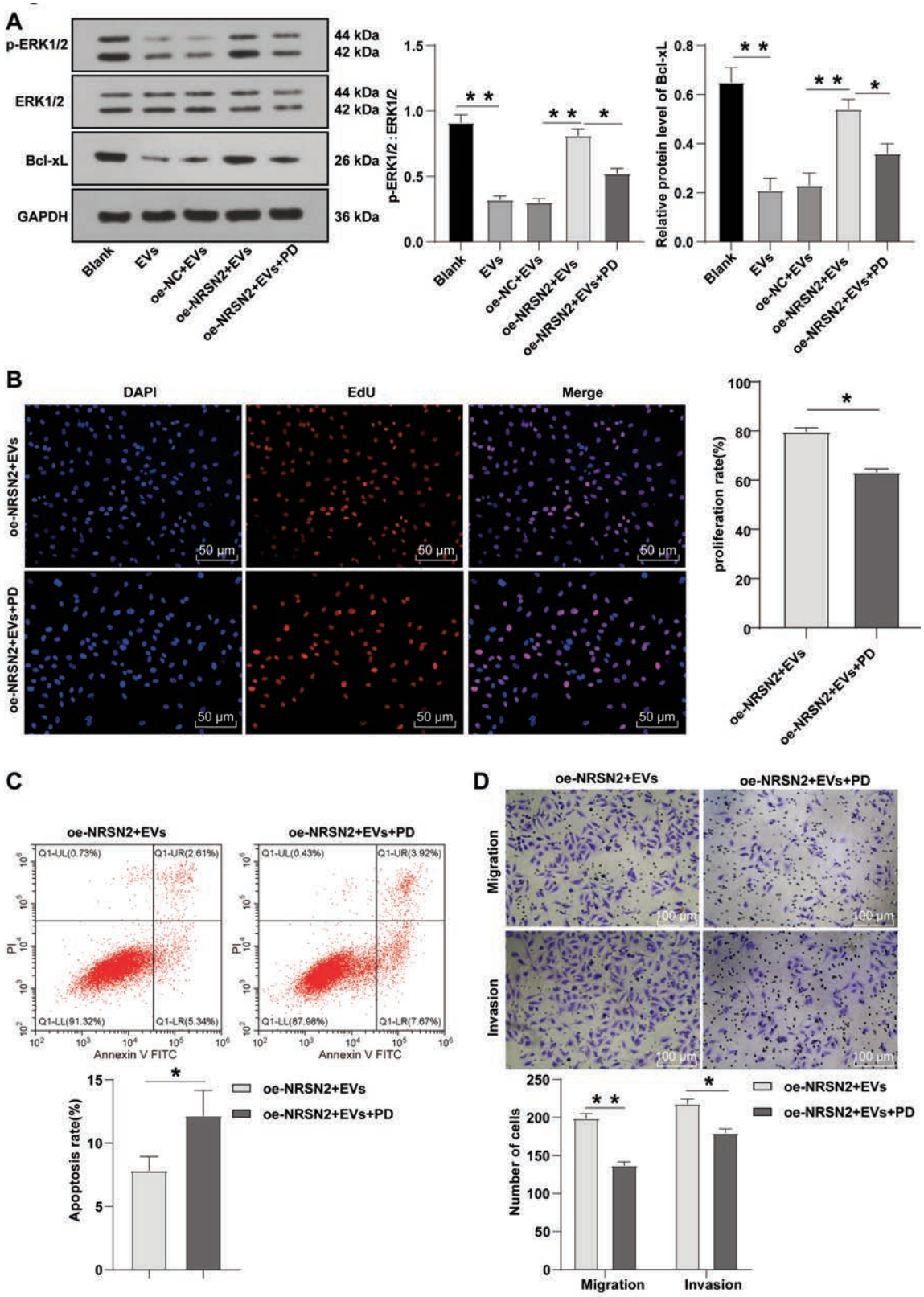

Figure 7. NRSN2 activated the ERK1/2-Bcl-xL signaling pathway to promote OS cell proliferation, migration, and invasion. After 24 h of EV treatment, NRSN2 overexpression treatment and 20 μM ERK1/2 specific inhibitor PD98059, WB showed that the levels of the ratio of p-ERK1/2:ERK1/2 and Bcl-xL protein were decreased (A); EdU assay demonstrated that proliferation rate was decreased (B); flow cytometry showed that apoptosis was increased (C); Transwell assay showed that cell migration (above) and invasion (below) were decreased (D). Three cell tests were performed and the data were expressed as mean ± SD. One-way ANOVA was used for comparison among groups (A) and independent *t*-test was used for comparison between two groups (B-D). Tukey's multiple comparisons test was used for *post-hoc* test; **p<0.01, *p<0.05.

progression of OS.[31] To further study the effect of NRSN2 on the downstream ERK1/2-Bcl-xL signaling pathway, it was found by WB analysis that the ratio of p-ERK1/2: ERK1/2 and Bcl-xL protein levels in OS cells were significantly downregulated after treatment with EVs. However, the ratio of p-ERK1/2: ERK1/2 and Bcl-xL protein levels were significantly upregulated after the overexpression of NRSN2 during EV treatment (all $p<0.01$) (Figure 7A). These results suggested that NRSN2 activated the ERK1/2/Bcl-xL pathway. Furthermore, the ERK1/2/Bcl-xL pathway was inhibited using PD98059. OS cell proliferation was decreased ($p<0.01$) (Figure 7B), cell apoptosis was increased ($p<0.01$) (Figure 7C), and cell migration and invasion were decreased (all $p<0.01$) (Figure 7D). The results above suggested that NRSN2 activated the ERK1/2/Bcl-xL pathway to promote OS cell malignant behaviors.

BMSCs-EVs inhibited the growth of OS in mice

The xenograft model of OS was established to study the role of BMSCs-EVs in tumor formation and progression. The experiments *in vivo* showed that compared with the control group, BMSC-EVs significantly reduced the growth rate, tumor volume, and weight of OS (all $p<0.01$) (Figure 8A-C). In addition, the results of immunohistochemistry showed that the proliferation of tumor cells (Ki-67) was significantly decreased after EVs treatment (Figure 8D). The tumor samples were detected by RT-qPCR. Compared with the control group, miR-206 was significantly upregulated and the expressions of NRSN2, the levels of the ratio of p-ERK1/2:ERK1/2 and Bcl-xL protein were significantly downregulated after EV treatment (all $p<0.01$) (Figure 8E-G). The results above suggested that BMSCs-EVs inhibited OS growth *in vivo*.

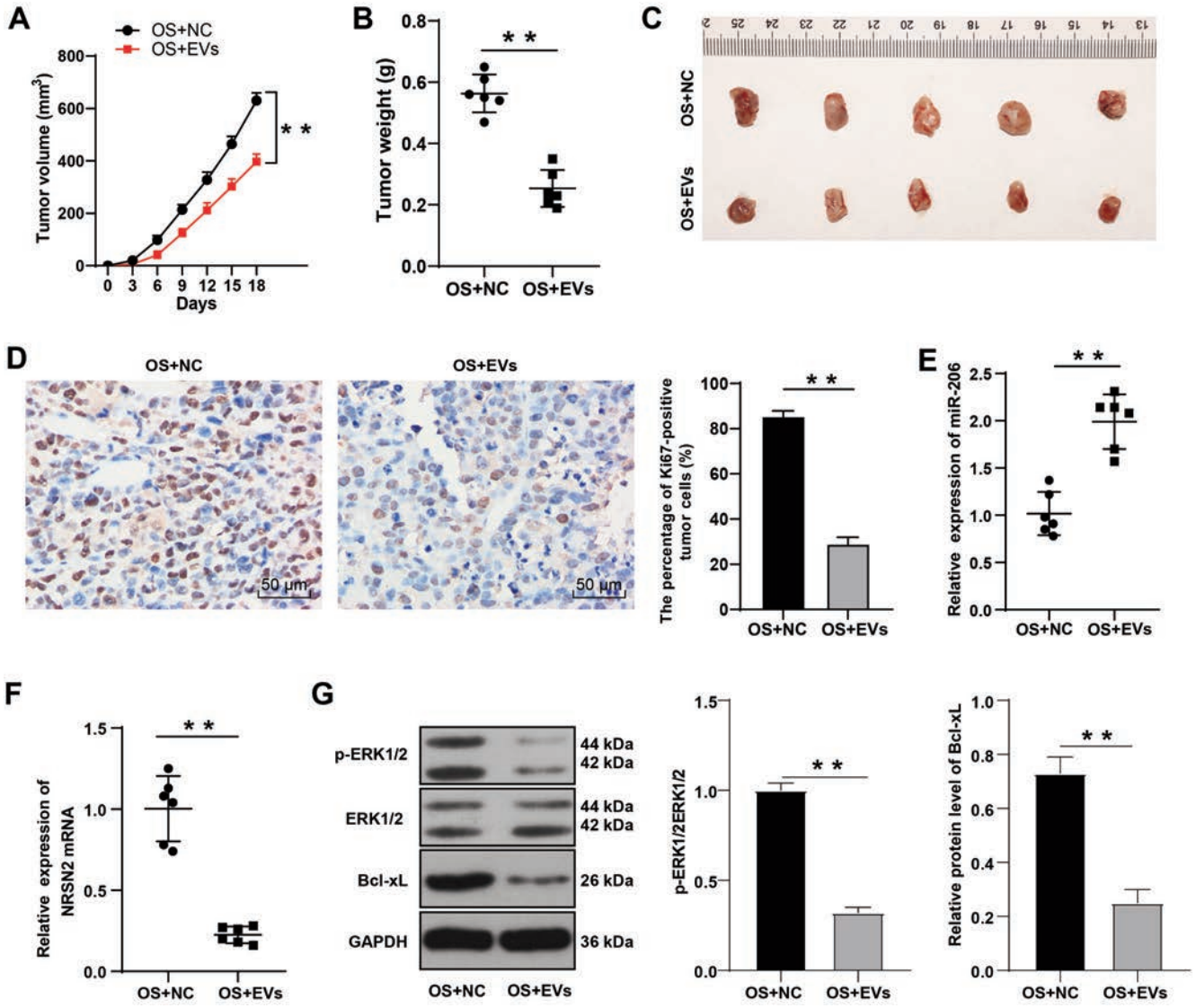

Figure 8. BMSCs-EVs inhibited the growth of OS in mice. After the xenograft model of OS was established, the OS mice were treated with BMSC-EVs. A-C) The growth rate, volume, and weight of tumors were decreased. D) Immunohistochemistry showed that the proliferation (Ki-67) of tumor cells was decreased. E-F) RT-qPCR demonstrated that the expressions of miR-206 was increased and NRSN2 mRNA was decreased. G) WB demonstrated that the expressions of p-ERK1/2, ERK1/2 and Bcl-xL, and levels of the ratio of p-ERK1/2:ERK1/2 and Bcl-xL protein were decreased were detected by WB; n=6; the data were expressed as mean ± SD. Independent *t*-test was used for comparison among groups; **p<0.01.

Discussion

OS is the most common primary malignant bone tumor.[3] The therapeutic management at present is a combined therapy of surgery and chemotherapy, which remains largely insufficient, as the survival of patients has not improved in recent decades.[39] EVs play a key role in intercellular communication in physiological and pathological environments, and evidence has shown that EVs are essential in the progression and metastatic process of OS.[40] This study found that BMSCs-EVs-shuttled miR-206 inhibited the activation of the ERK1/2-Bcl-xL pathway by targeting NRSN2, inhibited the proliferation, invasion, and migration of OS cells, and promoted apoptosis, thus inhibiting the progression of OS. This highlighted the potential value of BMSCs-EVs-shuttled miR-206 as a new therapeutic target for OS.

MSCs have important potential in regenerative medicine, which have effects on each component in the tumor microenvironment through autocrine or paracrine EVs to realize intercellular communication and can be modified and processed into good biological carriers for targeted therapy of OS.[41] EVs significantly weakened the proliferation, invasion, and migration of OS cells.[13,42,43] After coculture of BMSCs-EVs and 143B cells, we found EVs could be internalized by 143B cells, cell proliferation, invasion, and migration were inhibited, and apoptosis was promoted. It was consistent with the previous research results of EVs on OS.[44,45]

Circulating EVs encounter other cells and deliver miRNA cargo that leads to communication between different cells and is suggested to have a significant physiological effect.[46] The participation of miRNAs in OS has been extensively studied.[47-49] Increasing studies show that miR-206 is downregulated in various cancers, such as clear cell renal cell carcinoma,[50] head and neck squamous cell carcinoma,[21] and three negative breast cancer.[22] miR-206 is suppressed in OS.[13,23,24,37] GEO database analysis manifested that miR-206 was repressed in chip GSE28423 OS samples. High expression of miR-206 inhibited OS cell proliferation, which was related to the good prognosis of patients. miR-206 may be a potential target for OS therapy to improve early disease diagnosis.[25] The 143B cells were treated with EVs extracted from BMSCs before and after miR-206 inhibitor treatment. The miR-206 level in EVs-treated 143B cells was stimulated, cell proliferation, invasion, and migration were promoted, and apoptosis was reduced, while after miR-206 inhibitor treatment, the miR-206 levels in EVs and 143B cells were decreased, which partially annulled the inhibitory effects of EVs on the malignant behaviors of 143B cells. Consistently, miR-206 is downregulated in OS specimens, and miR-206 overexpression buffers OS carcinogenesis.[24]

NRSN2 is a small membrane protein located in the small vesicles of neural cells, which promotes the proliferation of OS cells.[27] BMSC-EVs promote proliferation, invasion, and migration of OS cells via the lncRNA MALAT1/miR-143/NRSN2/Wnt/β-catenin axis.[29] However, it has not been reported whether miR-206 plays an anti-cancer role in OS by regulating NRSN2. Starbase database and dual-luciferase assay elicited that there was a targeted binding relationship between miR-206 and NRSN2. Then, RT-qPCR showed that the mRNA level of NRSN2 in OS cells was augmented, and the level was the highest in 143B cells. After EV treatment, NRSN2 in OS cells was downregulated significantly, and NRSN2 expression was upregulated when miR-206 was inhibited in EVs. There is no report at present on the role of miR-206 and NRSN2. Moreover, we overexpressed NRSN2 in EVs-treated OS cells and found that after NRSN2 was overexpressed, the EVs effect on malignant behaviors of OS cells was reversed. In this study, we discovered that BMSCs-EVs shuttled miR-206 inhibited the proliferation, invasion and migration of OS cells and promoted apoptosis by targeting NRSN2 for the first time. The ERK1/2-Bcl-xL pathway mediates the apoptosis of OS cells.[30] Bcl-xL as a member of the Bcl-2 protein family acts as the dominant regulator of the death of apoptotic cells and plays principal roles in the tumor development and malignant transformation in OS.[51] Our results revealed that p-ERK1/2: ERK1/2 ratio and Bcl-xL expressions in OS cells were downregulated significantly after EV treatment, but upregulated after overexpression of NRSN2 during EV treatment. p-ERK1/2 and Bcl-xL expressions are upregulated in OS cells.[3]. There is little study on the relationship between NRSN2 and the ERK/Bcl-XL pathway. Furthermore, the ERK1/2/Bcl-xL pathway was inhibited using PD98059. OS cell proliferation was decreased, apoptosis was increased, and cell migration and invasion were decreased. This study initially showed that NRSN2 activated the ERK1/2-Bcl-xL pathway to promote OS cell malignant behaviors.

In summary, this study supported that BMSCs-EVs-shuttled miR-206 targeted NRSN2 and inhibited the ERK1/2-Bcl-xL pathway, thus inhibiting the malignant behaviors of OS cells. However, this study has some limitations. For example, this study only selected the OS cell line 143B with low miR-206 levels for related research and failed to select more cell lines for more extensive research, study the miR-206 level in clinical samples, and study other related mechanisms of the inhibitory effects of BMSCs-EVs on OS. More extensive and comprehensive research should be carried out in the future.

References

1. Hardes J, Gosheger G, Budny T. [Knochensarkome].[Article in German]. Z Orthop Unfall 2018;156:105-24.
2. Gill J, Ahluwalia MK, Geller D, Gorlick R. New targets and approaches in osteosarcoma. Pharmacol Ther 2013;137:89-99.
3. Mathkour M, Garces J, Beard B, Bartholomew A, Sulaiman OA, Ware ML. Primary high-grade osteosarcoma of the clivus: A case report and literature review. World Neurosurg 2016;89:730.e9-e13.
4. Biazzo A, De Paolis M. Multidisciplinary approach to osteosarcoma. Acta Orthop Belg 2016;82:690-8.
5. Kager L, Tamamyan G, Bielack S. Novel insights and therapeutic interventions for pediatric osteosarcoma. Future Oncol 2017;13:357-68.
6. Saraf AJ, Fenger JM, Roberts RD. Osteosarcoma: Accelerating progress makes for a hopeful future. Front Oncol 2018;8:4.
7. Whiteside TL. Exosome and mesenchymal stem cell cross-talk in the tumor microenvironment. Semin Immunol 2018;35:69-79.
8. Pegtel DM, Gould SJ. Exosomes. Annu Rev Biochem 2019;88:487-514.
9. Huang XY, Huang ZL, Huang J, Xu B, Huang XY, Xu YH, et al. Exosomal circRNA-100338 promotes hepatocellular carcinoma metastasis via enhancing invasiveness and angiogenesis. J Exp Clin Cancer Res 2020;39:20.
10. Barile L, Vassalli G. Exosomes: Therapy delivery tools and biomarkers of diseases. Pharmacol Ther 2017;174:63-78.
11. Baassiri A, Nassar F, Mukherji D, Shamseddine A, Nasr R, Temraz S. Exosomal non coding RNA in LIQUID biopsies as a promising biomarker for colorectal cancer. Int J Mol Sci 2020;21:1398.
12. Lan M, Zhu XP, Cao ZY, Liu JM, Lin Q, Liu ZL. Extracellular vesicles-mediated signaling in the osteosarcoma microenvironment: Roles and potential therapeutic targets. J Bone Oncol 2018;12:101-4.
13. Zhang H, Wang J, Ren T, Huang Y, Liang X, Yu Y, et al. Bone

marrow mesenchymal stem cell-derived exosomal miR-206 inhibits osteosarcoma progression by targeting TRA2B. Cancer Lett 2020;490:54-65.
14. Wang F, Li L, Piontek K, Sakaguchi M, Selaru FM. Exosome miR-335 as a novel therapeutic strategy in hepatocellular carcinoma. Hepatology 2018;67:940-54.
15. Wang Y, Zeng X, Wang N, Zhao W, Zhang X, Teng S, et al. Long noncoding RNA DANCR, working as a competitive endogenous RNA, promotes ROCK1-mediated proliferation and metastasis via decoying of miR-335-5p and miR-1972 in osteosarcoma. Mol Cancer 2018;17:89.
16. Ji Q, Xu X, Song Q, Xu Y, Tai Y, Goodman SB, et al. miR-223-3p inhibits human osteosarcoma metastasis and progression by directly targeting CDH6. Mol Ther 2018;26:1299-312.
17. Ren Z, He M, Shen T, Wang K, Meng Q, Chen X, et al. MiR-421 promotes the development of osteosarcoma by regulating MCPIP1 expression. Cancer Biol Ther 2020;21:231-40.
18. Shabani P, Izadpanah S, Aghebati-Maleki A, Baghbani E, Baghbanzadeh A, Fotouhi A, et al. Role of miR-142 in the pathogenesis of osteosarcoma and its potential as therapeutic approach. J Cell Biochem 2019;120:4783-93.
19. Wang S, Ma F, Feng Y, Liu T, He S. Role of exosomal miR21 in the tumor microenvironment and osteosarcoma tumorigenesis and progression (Review). Int J Oncol 2020;56:1055-63.
20. Zhang W, Wei L, Sheng W, Kang B, Wang D, Zeng H. miR-1225-5p functions as a tumor suppressor in osteosarcoma by targeting Sox9. DNA Cell Biol 2020;39:78-91.
21. Yan Y, Chang C, Su J, Veno M T, Kjems J. Osteoblastogenesis alters small RNA profiles in EVs derived from bone marrow stem cells (BMSCs) and adipose stem cells (ASCs). Biomedicines 2020;8:387.
22. Fei D, Sui G, Lu Y, Tan L, Dongxu Z, Zhang K. The long non-coding RNA-ROR promotes osteosarcoma progression by targeting miR-206. J Cell Mol Med 2019;23:1865-72.
23. Pan BL, Tong ZW, Wu L, Pan L, Li JE, Huang YG, et al. Effects of microRNA-206 on osteosarcoma cell proliferation, apoptosis, migration and invasion by targeting ANXA2 through the AKT signaling pathway. Cell Physiol Biochem 2018;45:1410-22.
24. Wang Y, Shi S, Zhang Q, Dong H, Zhang J. MicroRNA-206 upregulation relieves circTCF25-induced osteosarcoma cell proliferation and migration. J Cell Physiol 2020. Online ahead of print.
25. Xu X, Qiu B, Yi P, Li H. Overexpression of miR-206 in osteosarcoma and its associated molecular mechanisms as assessed through TCGA and GEO databases. Oncol Lett 2020;19:1751-58.
26. Zhang K, Dong C, Chen M, Yang T, Wang X, Gao Y, et al. Extracellular vesicle-mediated delivery of miR-101 inhibits lung metastasis in osteosarcoma. Theranostics 2020;10:411-25.
27. Keremu A, Maimaiti X, Aimaiti A, Yushan M, Alike Y, Yilihamu Y, et al. NRSN2 promotes osteosarcoma cell proliferation and growth through PI3K/Akt/MTOR and Wnt/beta-catenin signaling. Am J Cancer Res 2017;7:565-73.
28. Zhou J, Xu L, Yang P, Lu Y, Lin S, Yuan G. The exosomal transfer of human bone marrow mesenchymal stem cell-derived miR-1913 inhibits osteosarcoma progression by targeting NRSN2. Am J Transl Res 2021;13:10178-92.
29. Li F, Chen X, Shang C, Ying Q, Zhou X, Zhu R, et al. Bone marrow mesenchymal stem cells-derived extracellular vesicles promote proliferation, invasion and migration of osteosarcoma cells via the lncRNA MALAT1/miR-143/NRSN2/Wnt/beta-catenin axis. Onco Targets Ther 2021;14:737-49.
30. Zhang Z, Zheng Y, Zhu R, Zhu Y, Yao W, Liu W, et al. The ERK/eIF4F/Bcl-XL pathway mediates SGP-2 induced osteosarcoma cells apoptosis in vitro and in vivo. Cancer Lett 2014;352:203-13.
31. Sun T, Zhong X, Song H, Liu J, Li J, Leung F, et al. Anoikis resistant mediated by FASN promoted growth and metastasis of osteosarcoma. Cell Death Dis 2019;10:298.
32. Fu Y, Zhang L, Hong Z, Zheng H, Li N, Gao H, et al. Methanolic extract of Pien Tze Huang induces apoptosis signaling in human osteosarcoma MG63 cells via multiple pathways. Molecules 2016;21:283.
33. Trajkovic K, Hsu C, Chiantia S, Rajendran L, Wenzel D, Wieland F, et al. Ceramide triggers budding of exosome vesicles into multivesicular endosomes. Science 2008;319:1244-7.
34. Yue KY, Zhang PR, Zheng MH, Cao XL, Cao Y, Zhang YZ, et al. Neurons can upregulate Cav-1 to increase intake of endothelial cells-derived extracellular vesicles that attenuate apoptosis via miR-1290. Cell Death Dis 2019;10:869.
35. Wang X, Zhao X, Yi Z, Ma B, Wang H, Pu Y, et al. WNT5A promotes migration and invasion of human osteosarcoma cells via SRC/ERK/MMP-14 pathway. Cell Biol Int 2018;42:598-607.
36. Bao YP, Yi Y, Peng LL, Fang J, Liu KB, Li WZ, et al. Roles of microRNA-206 in osteosarcoma pathogenesis and progression. Asian Pac J Cancer Prev 2013;14:3751-5.
37. Ren D, Zheng H, Fei S, Zhao J L. MALAT1 induces osteosarcoma progression by targeting miR-206/CDK9 axis. J Cell Physiol 2018;234:950-7.
38. Zhan FB, Zhang XW, Feng SL, Cheng J, Zhang Y, Li B, et al. MicroRNA-206 reduces osteosarcoma cell malignancy in vitro by targeting the PAX3-MET axis. Yonsei Med J 2019;60:163-73.
39. Corre I, Verrecchia F, Crenn V, Redini F, Trichet V. The osteosarcoma microenvironment: A complex but targetable ecosystem. Cells 2020;9:976.
40. Perut F, Roncuzzi L, Baldini N. The emerging roles of extracellular vesicles in osteosarcoma. Front Oncol 2019;9:1342.
41. Chang X, Ma Z, Zhu G, Lu Y, Yang J. New perspective into mesenchymal stem cells: Molecular mechanisms regulating osteosarcoma. J Bone Oncol 2021;29:100372.
42. Qin F, Tang H, Zhang Y, Zhang Z, Huang P, Zhu J. Bone marrow-derived mesenchymal stem cell-derived exosomal microRNA-208a promotes osteosarcoma cell proliferation, migration, and invasion. J Cell Physiol 2020;235:4734-45.
43. Zhao W, Qin P, Zhang D, Cui X, Gao J, Yu Z, et al. Long non-coding RNA PVT1 encapsulated in bone marrow mesenchymal stem cell-derived exosomes promotes osteosarcoma growth and metastasis by stabilizing ERG and sponging miR-183-5p. Aging (Albany NY) 2019;11:9581-96.
44. Deng L, Wang C, He C, Chen L. Bone mesenchymal stem cells derived extracellular vesicles promote TRAIL-related apoptosis of hepatocellular carcinoma cells via the delivery of microRNA-20a-3p. Cancer Biomark 2021;30:223-35.
45. Ying H, Lin F, Ding R, Wang W, Hong W. Extracellular vesicles carrying miR-193a derived from mesenchymal stem cells impede cell proliferation, migration and invasion of colon cancer by downregulating FAK. Exp Cell Res 2020;394:112144.
46. Maciel E, Mansuy IM. Extracellular vesicles and their miRNA cargo: A means of communication between soma and germline in the mammalian reproductive system. Chimia (Aarau) 2019;73:356-61.
47. Kushlinskii NE, Fridman MV, Braga EA. Molecular mechanisms and microRNAs in osteosarcoma pathogenesis. Biochemistry (Mosc) 2016;81:315-28.

48. Ram Kumar RM, Boro A, Fuchs B. Involvement and clinical aspects of microRNA in osteosarcoma. Int J Mol Sci 2016;17:877.
49. Sekar D, Mani P, Biruntha M, Sivagurunathan P, Karthigeyan M. Dissecting the functional role of microRNA 21 in osteosarcoma. Cancer Gene Ther 2019;26:179-82.
50. Jia KG, Feng G, Tong YS, Tao GZ, Xu L. miR-206 regulates non-small-cell lung cancer cell aerobic glycolysis by targeting hexokinase 2. J Biochem 2020;167:365-70.
51. Wang ZX, Yang JS, Pan X, Wang JR, Li J, Yin YM, et al. Functional and biological analysis of Bcl-xL expression in human osteosarcoma. Bone 2010;47:445-54.

Received for publication: 10 February 2022. Accepted for publication: 27 April 2022.

European Journal of Histochemistry 2022; 66:3394
doi:10.4081/ejh.2022.3394